Slow magnetic relaxation in a heteroleptic anilate-based Dy III metal–organic framework

Mariangela Oggianu, Federica Bertolotti, Fabio Manna, Francesco Congiu, Antonio Cappai, Claudio Melis, Giorgio Concas, Narcis Avarvari, Norberto Masciocchi, Maria Laura Mercuri

ChemComm

COMMUNICATION

Slow MagneticRelaxation in a Heteroleptic Anilate-based Dy^{III} Metal-Organic Framework

Received 00th January 20xx,
Accepted 00th January 20xx

DOI: 10.1039/x0xx00000x

Mariangela Oggianu,[ac] Federica Bertolotti[e], Fabio Manna[bc], Francesco Congiu[d], Antonio Cappai[d], Claudio Melis[d], Giorgio Concas[d], Narcis Avarvari,[b] Norberto Masciocchi[e] and Maria Laura Mercuri*[ac]

Novel heteroleptic anilate-based lanthanide MOFs (Ln^{III}= Tb, Dy, Ho) have been obtained under hydrothermal conditions by the ancillary ligand synthetic strategy. These structurally isomorphous speciescontain octacoordinated Ln^{III} ionswith coordination polyhedra approaching an ideal D_{2d}symmetry, best described by a distorted biaugmented trigonal prismatic C_{2v} geometry. In the whole series,only Dy-MOF exhibits SMM behaviour.

Metal-Organic Frameworks (MOFs), porous materials formed by the self-assembling of organic ligands (linkers) and metal ions (nodes) have attracted considerable attention in several fields, spanning from gas separation, catalysis, sensing, molecular electronics to biomedicine.[1–3]In particular, MOFs exhibiting Single-Molecule Magnetbehaviour (SMMs) have received an ever growing interest for potential applications in molecular spintronics and quantum computing devices.[4]Ln^{III} ions, and especiallyTb^{III} and Dy^{III},are the best candidates to construct Lanthanide MOFs (Ln-MOFs) with SMMs properties,[5,6]thanks to their large magnetic anisotropy by virtue of the strong angular dependence of *4f* orbitals.Ln-MOFs, in which the coordination geometry of the Ln^{III} ion is approximately square-antiprismatic or bidisphenoidal (overall,Δ-dodecahedral), are potential candidates as Single Ion Magnets (SIMs), a second generation of SMMs-based MOFs formed by single centres that exhibit slow magnetic relaxation.[7] In this respect, the distortion of the coordination environment of the Ln^{III} ions depends on the number and nature of additional/ancillary linkers and on often unpredictable intermolecular interactions in the crystal phase. These fundamental aspects, affecting the magnetic relaxation behaviour, make rather crucial all steps in the design of a SIM-MOF, such as the choice of:i)thebuilding blocks, ii) the solvents and iii) the overall synthetic procedure. Within the large class of multitopic organic linkers present in the literature, those based on the 2,5-dihydroxy-1,4-benzoquinone *core*, and usually called anilates, have been extensively employed, by us and others, in the preparation of Ln^{III}-based coordination polymers and MOFs. [8–11]The presence of strong magnetic exchange interactions through the *exo*-bis-bidentate ligand and their favourable redox ability make indeed anilate-based linkers suitable candidates for the construction of materials showing SIM behaviour.[12–16]We have recently reported on the synthesis and completecharacterization of 3D Ln-MOFs based on 3-chloro-6-cyano-2,5-dihydroxy-1,4-benzoquinone (KHClCNAn) and tetrafluoro-terephthalic acid (H_2F_4BDC), formulated as $[Yb_2(\mu\text{-ClCNAn})_2(\mu\text{-}F_4BDC)(H_2O)_4]\cdot 3H_2O$ and $[Er_2(\mu\text{-ClCNAn})_2(\mu\text{-}F_4BDC)(H_2O)_4]\cdot 4H_2O$,[17] obtained under hydrothermal conditions by using the ancillary ligand strategy. Through a similar approach, by reacting KHClCNAn and $H_2F_4BDC$with Tb^{III}, Dy^{III} and Ho^{III} ions, a new family of 3D MOFs, formulated as $[Ln_2(\mu\text{-ClCNAn})_2(\mu\text{-}F_4BDC)(H_2O)_4]\cdot 4H_2O$ [Ln^{III} = Tb (**1**); Dy (**2**); Ho (**3**)] have been obtained. Their structural characterization, performed by a combination of single-crystal(**1**) and powder X-ray (PXRD) diffraction methods (**2** and**3**), indicated a distorted biaugmented trigonal prismatic C_{2v} geometry, whichslightly deviates from the ideal D_{2d} polyhedral geometry.

Compounds **1**, **2** and **3** were obtained by combining Tb^{III}, Dy^{III} and Ho^{III}ionswith two distinct organic linkers, $ClCNAn^{2-}$ and F_4BDC^{2-}, under hydrothermal conditions. This method allowed to directly isolate 3D frameworks. At variance, one-pot synthesis or layering techniques, usingthe same reagents, resulted in 2D coordination polymers,[9,10] corroborating the idea that 3D Ln-MOF structures are more easily formed under solvothermal conditions.[17]Compound **1** crystallizes in the centrosymmetric triclinic *P-1* space group andis isomorphous to the already known Yb^{III} and Er^{III}derivatives.‡ The asymmetric unit of **1**(see Figure 1) contains one Tb^{III}ion, two half chlorocyananilatemoieties and one half tetrafluoro-terephtalateligand, two coordinated water molecules and two loosely bound water molecules within 1D channels (*vide infra*)

[a] *Dipartimento di ScienzeChimiche e Geologiche, Università degli Studi di Cagliari, 09042 Monserrato, Italy.*
[b] *Univ Angers, CNRS, MOLTECH-ANJOU, SFR MATRIX, F-49000 Angers, France.*
[c] *INSTM, Via Giuseppe Giusti, 9, 50121 Firenze, Italy*
[d] *Dipartimento di Fisica, Universitàdegli Studi di Cagliari,09042 Monserrato, Italy.*
[e] *Dipartimento di Scienza e Alta Tecnologia&To.Sca.Lab., Università dell'Insubria, via Valleggio 11, 22100 Como, Italy.*

† Footnotes relating to the title and/or authors should appear here.

*Corresponding author: e-mail mercuri@unica.it

Electronic Supplementary Information (ESI) available: [details of any supplementary information available should be included here]. See

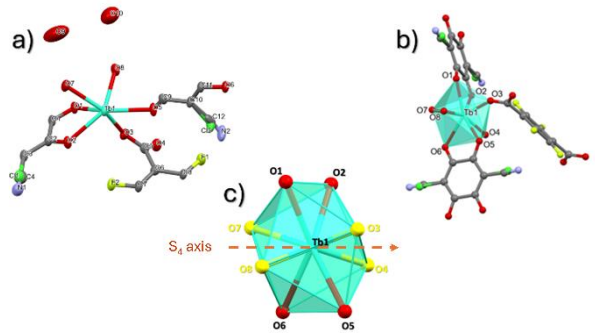

Figure 1. Thermal ellipsoid representation of the asymmetric unit within species **1**; b) a polyhedral representation of the full coordination environment; c) representation of the coordination polyhedron about Tb^{III}. Color codes: C grey, N blue, O red, F yellow, Cl green, Tb cyan, H atoms were omitted for clarity. The dashed arrow in panel c) indicates the idealized S_4 axis of a D_{2d} coordination polyhedron.

The chloro and cyano substituents, present in the 1,4 positions of the non-centrosymmetric $ClCNAn^{2-}$ ligand, by virtue of their similar electronic requirements and steric hindrance, are disordered and required the use of site occupancy factors of 0.5, which appears to be a rather common feature for this linker.[17] Tb^{III} is octa-coordinated, with the coordination sphere composed by four O atoms from two different anilate linkers, two O atoms from two different carboxylate linkers and two water molecules. As a first approximation, the geometry about the Tb^{III} ion is bisphenoidal with idealized D_{2d} symmetry. Tb-O bond distances, supplied in Table S1, show that they fall into a surprisingly narrow range, only 0.18 Å wide; the two Tb-O_{water}links are shorter than other Tb-O bonds, as if the Lewis basicity of (some of) the C-bound oxygen atoms was lowered by the presence of electron-withdrawing residues, or, more likely, as if stereochemical constraints of the chelating anilate moieties were at work. Among the many known octa-coordinated coordination polyhedra, the Continuous Shape Measurement (CShM) model, implemented in the Shape2.1 software,[18] suggests that the coordination geometry of Tb^{III} in **1** is best described by a C_{2v}distorted biaugmented trigonal prism with aCShM value of 7.132; the second best polyhedron, with a slightly higherCShM value of 7.813, is the D_{2d}bisdisphenoid (the Δ-dodecahedron), which we prefer to use in the following discussion. Figure 1c highlights this choice, where the main axis is horizontaland the two intertwined sphenoids are separated by color codes, red for the ”equatorial” one and yellow for the “axial” one.

Worthy of note, the water ligands (O7 and O8) belong to the latter, whereas both couples of “red” oxygens belong to the chelating anilates. The (short enough) C-O distances (4×), falling near 1.25 Å, confirm the delocalized character of theanilate ligand and the substantial equivalence of all carbonyls.

Thanks to the μ_2,η^4 bridging mode of the anilate ligand connecting Tb^{III} ions along infinite 1D chains (running in the [011] direction), branching out along [01-1] through the tetradentate *exo*-bis-bidentate F_4BDC^{2-} anions, a 3D polymeric network with a **mog** topology is formed (Figure 2).[19]

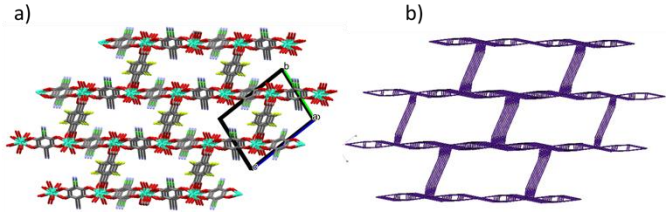

Figure 2. a) Capped-stick representation of the porous network of **3**, obtained by omitting the loosely bound water and all H atoms; the orientation of the unit cell is also shown, highlighting the presence of a brickwall motif normal to the (short) **a** axis. b) representation of the **mog** topology with Topospro.Color codes: C grey, N blue, O red, F yellow, Cl green and Tb cyan.

Such crystal packing allows the formation of 1D channels of nearly rectangular section, which are filled by water molecules. Omitting from the structural model these loose water molecules provides channels in which spheres with (up to) 1.80 Å radii can be allocated, for a 19.2% accessible volume (calculated with Olex2, see Figure S1).[20]

According to the lattice parameters derived from PXRD data shown in Figure 3a and collected in Table S3, compounds **2** and **3**, $[Ln_2(\mu\text{-}ClCNAn)_2(\mu\text{-}F_4BDC)(H_2O)_4]\cdot 4H_2O$[$Ln^{III}$ = Dy, Ho], are fully isomorphous, no matter what the correct formulation of the poorly detectable unbound water moieties is. These are indeed loosely located in the crystal lattice within the voids generated by infinite 2D channels running parallel to the **a** axis, accounting for a significant 16% of the total volume. This structural feature likely makes their actual occurrence and quantity highly dependent on environmental conditions, mostly temperature and relative humidity. Their nature, thus, closely resembles the so-called non-stoichiometric “channel hydrates”, which have raised the interest of many, particularly in the pharmaceutical field.[21] On this basis, it should not surprise that Yb^{III} and Er^{III} basedspecies have been formulated with different water contents. Nevertheless, our geometrical analysis, shown in Figure 3b, evidences a robust correlation between cell volumes and crystal radii (taken from Shannon’s tables)[22] and manifests the absence of sizable inflation effects attributable to the insertion of unpredictable amounts of weakly bound water molecules.

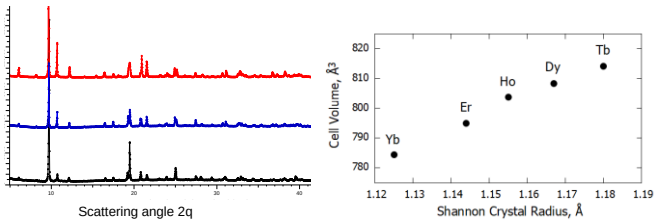

Figure 3. Left: Synoptic plot of the PXRD data for species **1**(black trace), **2**(blue) and **3**(red), demonstrating their isomorphous nature; *y*-axis: intensity (a.u). PXRD patterns are vertically shifted to improve readability. Right: Cell volume dependence on the size of the Ln^{III} ions (R^2 = 0.987).

The direct current (DC) magnetic susceptibility (χ) vs. temperature (T) was measured for all compounds (see Figure S3). The r.t. value of χT (Table 1) is in good agreement with the expected values for magnetically isolated Tb, Dy and Ho ions (11.82, 14.17 and 14.07 $cm^3 \cdot K\ mol^{-1}$, respectively).[23] As the temperature decreases, χTfollows Curie's law down to about 150 K.[23] Below 150 K, χT values decrease, as expected for highly anisotropic magnetic centers, due to a selective depopulation of the excited Stark levels.[24,25] Stark effect-induced splitting of these levels is due to the crystal field generated by the oxygen atoms of the Ln-coordination polyhedron.

Density Functional Theory (DFT) calculations, taking into account the periodicity of the lattice, were performedusingQuantumEspressoand aplane wave basis set and pseudopotentials.[26] All calculations were performed in spin-polarized mode to account for possible spin effects. The experimental structure was first optimized by fully relaxingthe lattice metrics and all atomic positions. Then, the electronic charge densityand the formal charge of the oxygen atoms were calculated (Table S4), and used to evaluate the crystal field for the Dy^{III}ion. This fieldforms an angle of about 13° with the S_4symmetry axis shown in Figure1c and of about 81° and 86° with the two C_2 axes normal to it, pointing towards the O7 and O8 atoms. The field is axial with good approximation. For oblate ions like Dy^{III}, the axial field favours a highly anisotropic ground state and SMM behaviour.[27]The analytical expression of the Dy^{III} susceptibility is given in Eq. S1..[28] The zero field splitting parameter (Δ) is defined by the Hamiltonian in zero magnetic field $H = -\Delta J_z^2$, neglecting the higher order term.[29,30]Eq. S1 was used to fit the susceptibility data of **2** in the 50–300 K temperature range used in the literature;[24,25] the same procedure was followed for compounds **1** and **3** (Eqs. S2 and S3).The curve fitting, shown in Figures S3-S6, provided the g and Δ parameters reported in Table 1. The g values are in good agreement with the theoretical ones (1.50, 1.33 and 1.25 for trivalent Tb^{III}, Dy^{III} and Ho^{III} ions [23]) and the Δ values are comparable with literature data for Tb^{III}, Dy^{III} and Ho^{III}SMMs.[24,28]The introduction of the intermolecular magnetic interaction between Ln ions, based on the molecular fied approximation, does not improve the fit.[28]

The DC magnetization *vs*. applied field was measured from 2 K to 10 K at2 K steps. The curves for fields from 2 to 90 kOe as a function of field/temperature ratio are shown in FiguresS7-S9, whereas the magnetizations vs. applied fieldat 2 K are included in FigureS10. Magnetization does not saturate even at 2 K and 90 kOe,withthe numbers of Bohr magnetons (see Table 1) smaller than the theoretical ones(9, 10 and 10$\mu_B$for Tb^{III}, Dy^{III} and Ho^{III}[23]), confirming the high magnetic anisotropy of these single ions.[25]In order to explore potential SMM behaviour, alternating current (AC) magnetic susceptibility measurements werecarried out on the three compounds as a function of both temperature and frequency, in both zero and non-zero DC applied fields. For compound **2**, under zero DC

field no peak was observed in the out-of-phase (χ'') susceptibility (Figure S11b).When an external DC field (H_{DC} = 1000 Oe) was applied, a peak appearedin χ'' below 10 K

Table 1. DC susceptibility times temperature at 300 K (χT_{300}), best fit parameters (Landé g-factor$g$ and zero field splitting parameter Δ) and number of Bohr magnetons (n_B) at 2 K and 90 kOe.

Compound	χT_{300}	g	Δ (cm^{-1})	n_B
1(Tb)	12.5	1.57	0.39	6.3
2(Dy)	14.9	1.25	0.11	6.6
3(Ho)	14.7	1.30	0.23	6.5

(Figure S11d). FigureS12 shows the effect of the increasing H_{DC}, where 5000 Oe appears to be the best value: we therefore analysed the dynamic susceptibility response with this applied field. At H_{DC} = 5000 Oe, **2** shows a clear, frequency dependent,$\chi''(T)$ peak around 8 K (Figures 4 and S11f), which is a marker for SMM behaviour.[24,25]The same sequence of events was observed in $\chi'(T)$ (Figures S11a,c,e and S12a).The requirement of an external magnetic field to observe this behaviour indicates the presence of fast relaxation due to quantum tunnelling of magnetization (QTM).[25,31]The shift of the peak temperature (T_p) of $\chi''(T)$ fora given frequency (ν)difference, for the adjacent pairs of frequencies in the range 1.335 – 10 kHz,can be analyzed in terms of the parameter $\Phi = (\delta T_p/T_p)/\delta\log(\nu)$. We obtained Φ = 0.29, *i.e.* within the $0.1<\Phi<0.3$ range, as expected for SMMs.[32]This magnetization relaxation process can be examined according to Debye's model with the relaxation time following Arrhenius' law (Orbach process), by applying the Eq. S4[25,29]for a frequency of 10 kHz; from the fit (FigureS13) we obtained an energy barrier U_{eff} = 12.6 K and a relaxation time $\tau_0 = 1.4 \times 10^{-7}$ s, in line with literature data.[25]

Cole-Cole plots were studied reporting χ''*vs.*χ' at different temperatures in the 2– 5 K range(FigureS14). The single arc curveswere fitted according to the generalized Debye model (see Eqs. S5 and S6[29]). The fitting parameters obtained in the 20 -2615Hzfrequency range are givenin TableS5; the values of theparameter accounting for the spread of relaxation times(α) fall in the 0.28 - 0.47range, as found elsewhere.[24] Similar AC magnetization measurements were performed on compounds **1** and **3**, but no peaks in the $\chi''(T)$ curves(FiguresS15 and S16), characterizing SMMs, were observed.

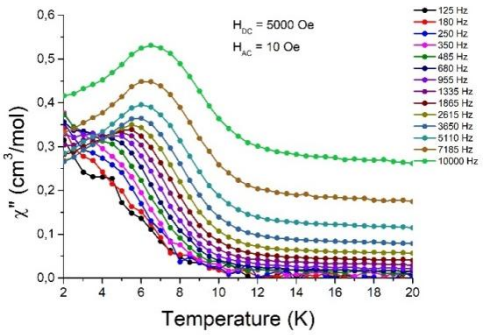

Figure 4. Temperature dependence of the out of phase χ" component for compound **2** (Dy) measured under H_{DC} = 5000 Oe in the frequency range 125 Hz - 10 kHz

In summary,within the new family of heteroleptic 3D lanthanide MOFs here presented, only compound **2** (Dy)

showsan evident SMM behaviour.Theoretical calculations enabled the evaluation ofthe crystal field for the Dy^{III} ion from the calculated charges, which is axial, polar and aligned with the principal axis of the coordination polyhedron. In the case of the structurally isomorphous species **1** and **3**, slightly different (yet undetected) stereochemical distortions from the ideal D_{2d} polyhedral geometry may be detrimental for SMM behaviour.Remarkably the ancillary linker is crucial in determining the geometry of the Ln^{III} ions approaching an ideal D_{2d} symmetry and thus in the observed SMM behaviour, differently from the paramagnetic Dy-compounds already reported by some of us.[9]

This work was supported by the Fondazione di Sardegna (FDS, project F73C23002170007) and the CNRS and the University of Angers. Special thanks are due to Dr. Magali Allain (MOLTECH-ANJOU, Angers).

Conflicts of interest

There are no conflicts to declare.

Notes and references

‡The CIF file for compound **1** has been deposited at the Cambridge Structural Database with CCDC N. 2355664.

1 D. Hu, J. Zhang and M. Liu, *Chem. Commun.*, 2022, **58**, 11333–11346.

2 N. Monni, E. Andres-Garcia, K. Caamaño, V. García-López, J. M. Clemente-Juan, M. Giménez-Marqués, M. Oggianu, E. Cadoni, G. Mínguez Espallargas, M. Clemente-León, M. L. Mercuri and E. Coronado, *J. Mater. Chem. A*, 2021, **9**, 25189–25195.

3 M. Oggianu, N. Monni, V. Mameli, C. Cannas, S. A. Sahadevan and M. L. Mercuri, *Magnetochemistry*, 2020, **6**, 1–14.

4 N. Monni, J. J. Baldoví, V. García-López, M. Oggianu, E. Cadoni, F. Quochi, M. Clemente-León, M. L. Mercuri and E. Coronado, *Chem. Sci.*, 2022, **13**, 7419–7428.

5 F. Gendron, B. Pritchard, H. Bolvin and J. Autschbach, *Dalt. Trans.*, 2015, **44**, 19886–19900.

6 F. Manna, M. Oggianu, N. Avarvari and M. L. Mercuri, *Magnetochemistry*, , DOI:10.3390/magnetochemistry9070190.

7 B. Fernández, I. Oyarzabal, E. Fischer-Fodor, S. MacAvei, I. Sánchez, J. M. Seco, S. Gómez-Ruiz and A. Rodríguez-Diéguez, *CrystEngComm*, 2016, **18**, 8718–8721.

8 S. A. Sahadevan, N. Monni, A. Abhervé, G. Cosquer, M. Oggianu, G. Ennas, M. Yamashita, N. Avarvari and M. L. Mercuri, *Inorg. Chem.*, 2019, **58**, 13988–13998.

9 S. Ashoka Sahadevan, N. Monni, M. Oggianu, A. Abhervé, D. Marongiu, M. Saba, A. Mura, G. Bongiovanni, V. Mameli, C. Cannas, N. Avarvari, F. Quochi and M. L. Mercuri, *ACS Appl. Nano Mater.*, 2020, **3**, 94–104.

10 S. Ashoka Sahadevan, F. Manna, A. Abhervé, M. Oggianu, N. Monni, V. Mameli, D. Marongiu, F. Quochi, F. Gendron, B. Le Guennic, N. Avarvari and M. L. Mercuri, *Inorg. Chem.*, 2021, **60**, 17765–17774.

11 M. Oggianu, A. Abhervé, D. Marongiu, F. Quochi, J. R. Galán-Mascarós, F. Bertolotti, N. Masciocchi, N. Avarvari and M. L. Mercuri, *Molecules*, , DOI:10.3390/molecules28186453.

12 S. Benmansour and C. J. Gómez-García, *Magnetochemistry*, 2020, **6**, 1–44.

13 K. Bondaruk and C. Hua, *Cryst. Growth Des.*, 2019, **19**, 3338–3347.

14 A. Hernández-Paredes, C. Cerezo-Navarrete, C. J. Gómez García and S. Benmansour, *Polyhedron*, 2019, **170**, 476–485.

15 Y. Wang, X. Liu, X. Li, F. Zhai, S. Yan, N. Liu, Z. Chai, Y. Xu, X. Ouyang and S. Wang, *J. Am. Chem. Soc.*, 2019, **141**, 8030–8034.

16 B. F. Abrahams, J. Coleiro, K. Ha, B. F. Hoskins, S. D. Orchard and R. Robson, *J. Chem. Soc. Dalt. Trans.*, 2002, **2**, 1586–1594.

17 M. Oggianu, F. Manna, S. A. Sahadevan, N. Avarvari, A. Abhervé and M. L. Mercuri, *Crystals*, , DOI:10.3390/cryst12060763.

18 S. Alvarez, P. Alemany, D. Casanova, J. Cirera, M. Llunell and D. Avnir, *Coord. Chem. Rev.*, 2005, **249**, 1693–1708.

19 V. A. Blatov, A. P. Shevchenko and D. M. Proserpio, *Cryst. Growth Des.*, 2014, **14**, 3576–3586.

20 O. V. Dolomanov, L. J. Bourhis, R. J. Gildea, J. A. K. Howard and H. Puschmann, *J. Appl. Crystallogr.*, 2009, **42**, 339–341.

21 E. Jurczak, A. H. Mazurek, Ł. Szeleszczuk, D. M. Pisklak and M. Zielińska-Pisklak, *Pharmaceutics*, 2020, **12**, 1–25.

22 B. Y. R. D. Shannon, M. H, B. N. H, G. O. H, M. Eu and V. Cu, *October*.

23 N. D. Ashcroft, N. W.; Mermin, *Solid State Physics*, Andover, 1976.

24 U. Huizi-Rayo, A. Zabala-Lekuona, A. Terenzi, C. M. Cruz, J. M. Cuerva, A. Rodríguez-Diéguez, J. A. García, J. M. Seco, E. San Sebastian and J. Cepeda, *J. Mater. Chem. C*, 2020, **8**, 8243–8256.

25 E. Echenique-Errandonea, R. F. Mendes, F. Figueira, D. Choquesillo-Lazarte, G. Beobide, J. Cepeda, D. Ananias, A. Rodríguez-Diéguez, F. A. Almeida Paz and J. M. Seco, *Inorg. Chem.*, 2022, **61**, 12977–12990.

26 P. Giannozzi, O. Andreussi, T. Brumme, O. Bunau, M. B. Nardelli, M. Calandra, R. Car, C. Cavazzoni, D. Ceresoli, M. Cococcioni and others, *J. Phys. Condens. Matter*, 2017, **29**, 465901.

27 T. G. Ashebr, H. Li, X. Ying, X.-L. Li, C. Zhao, S. Liu and J. Tang, *ACS Mater. Lett.*, 2022, **4**, 307–319.

28 J. Cepeda, R. Balda, G. Beobide, O. Castillo, J. Fernández, A. Luque, S. Pérez-Yáñez, P. Román and D. Vallejo-Sánchez, *Inorg. Chem.*, 2011, **50**, 8437–8451.

29 C. V. Topping and S. J. Blundell, *J. Phys. Condens. Matter*, , DOI:10.1088/1361-648X/aaed96.

30 J. J. Baldoví, E. Coronado, A. Gaita-Ariño, C. Gamer, M. Giménez-Marqués and G. Mínguez Espallargas, *Chem. - A Eur. J.*, 2014, **20**, 10695–10702.

31 S. Jiang, B. Wang, G. Su, Z. Wang and S. Gao, *Angew. Chemie*, 2010, **122**, 7610–7613.

32 Y. J. Ma, J. X. Hu, S. De Han, J. Pan, J. H. Li and G. M. Wang, *J. Am. Chem. Soc.*, 2020, **142**, 2682–2689.

